Identification of dynamic nonlinearities of bolted structures using strain analysis

C. Blandin, D. Di Maio

Dario Di Maio, University of Bristol, UK

C. Blandin, University of Bristol, UK

ABSTRACT

This work investigates the identification of the nonlinear behaviour of bolted structures through experimental and numerical analysis. Friction joints (especially bolted joints) generate nonlinear dynamic behaviours in a bolted assembled structure subject to dynamic loadings (especially high level vibrations) due to energy dissipation. The causes of nonlinearities are multiple and the ones related to joints will be researched in this piece of work. Although numerical simulation of nonlinear dynamic behaviour is complex, Finite Element models of a bolted flange will be used for strain analysis in order to develop a strategy for test planning of nonlinear vibration testing. Experimental tests and parameters that can be used to identify the joint nonlinearities will be used for developing correlation methods.

KEYWORDS: Modal testing, joints, nonlinearity, strain

1 INTRODUCTION

Bolted assemblies are widely used in the mechanical industry. Understanding their dynamic behaviour is critical in a design process. Most of bolted assemblies used in engines (especially aircraft gas turbines) are subject to high levels of vibrations. Then, it is necessary to understand how the structure behaves under such loading conditions. Both numerical and experimental modal analysis have been well known and used for decades in the mechanical industries [1], allowing to predict the structure response subject to dynamic loadings. However, most of those analyses are performed under linear conditions, which can be applied in most of the cases. But in the case of bolted assemblies, the friction joint dynamic behaviour generally can induce some nonlinearities in the structure response from a certain level of vibration. Then, the classic linear approach cannot be used anymore.

A literature review [2] has been achieved in order to give an insight of the dynamic nonlinearities of bolted structures from an experimental, analytical and numerical points of view. First, we tried to explain the main physical phenomena behind the joint nonlinearities. The main factors that lead to this nonlinear behaviour are the friction phenomena and the clapping (micro-impacts) that can occur in case of looseness in the joint according to R.A. Ibrahim and C.L. Pettit [3]. The former cause comes from the sliding and sticking states in the contact surface area due to a complex shear stress field and a non-uniform contact pressure applied by the bolts as it has been shown by Yaxin Song, D. Michael McFarland, Lawrence A. Bergman, and Alexander F. Vakakis [4]. The localised zones being in sliding state are called microslip zones. They induce coulomb friction energy dissipation, resulting in force-displacement hysteresis loops, as it has been shown by S. Bograd, P.Reuss, A.Schmidt, L.Gaul,

M.Mayer [5]. This energy dissipation has an effect on the damping in the structure dynamics. Indeed, two forms of damping can be identified: the structural damping due to the material characteristics, and the dry friction damping due to the energy dissipation in the bolted joint. For simple Single Degrees Of Freedom (SDOF) systems, this friction damping increases with an increasing level of vibration (or excitation force). The stiffness of the structure is also affected and decreases with an increasing level of vibrations. These affect the Frequency Response Function (FRF) of the system.

As previously said, in a design process, it is critical to predict the dynamic response of an assembled structure. However, even nowadays, bolted surfaces are assumed to be glued in most FEM, which is an assumption only valid for low levels of vibrations. Many analytical and numerical models have been developed to predict the nonlinear dynamical behaviour of bolted assembled systems and are referenced in the literature review. Thanks to the development of FEA and computational capabilities, it is today possible to implement the joint characteristics in a numerical model. There are several ways to do so, some are more accurate although there are more computational consuming and some are easier to implement and faster to solve, but generally less accurate. A first method consists in implementing contact elements such as Iwan elements [7] or Valanis models [8] usually composed of springs and coulomb friction elements are able to predict an accurate response of a bolted structure, but they are very computational consuming. Another technique developed by H. Ahmadian, M. Ebrahimi, J.E. Mottershead and M.I. Friswell [9] consists in inserting a thin-layer of nonlinear elements between the two surfaces in contact. It has the advantage of solving the numerical model faster, but it requires a complex parameters updating with experimental data.

In modal analysis, a correlation between experimental and numerical data is often required to update the FEM, even in linear conditions (low vibration levels). Indeed, many parameters have a great sensitivity on the frequency response, such as the structural damping and the joint parameters (bolt preload, friction coefficient, etc). An algorithm is generally used as an optimization function to update the numerical FRF (generally obtained with a Harmonic Balance Method) and the experimental FRF, as it has been shown by Marc Böswald and Michael Link [10].

From an experimental point of view, most papers about bolted joint nonlinearities are about single degrees of freedom systems which require a minimum amount of sensors, having a limited residual effect on the structure response. However, for industrial structures, which can have a large number of degrees of freedom, specific experimental techniques must be used to avoid a change in behaviour too important due to sensors glued to the structure. These techniques, such as laser vibrometer measurements [11] are contactless, avoiding any potential structural perturbation from the measurement material.

In the aerospace industry, many revolution components from the engine are assembled by flange bolted joints which are likely to induce some dynamic nonlinearities as it has been previously explained earlier. For several years, it has become an important research field from the gas turbine industry. Particularly, the nonlinearities caused by contact interactions between engine parts have just begun to be better understood. For example, in this seminar, E. Chatelet proposed a contact area identification process using full-field displacement surface measurements in a simple structure subject to harmonic forcing of different levels [12]. In this study, we will particularly focus on the Combustion Chamber Outer Casing (CCOC) and High Pressure Chamber (HPC) from a Rolls-Royce engine (see Figure 1) which is assembled using a bolted flange. For these complex structures containing a large number of degrees of freedom, the joint nonlinearity is mode dependant, as it has been introduced by C. Schwingshackl, D. Di Maio and I. Sever [6]. That is to say, the nonlinearity can be more or less important regarding the excited mode. The aim of this research is to study this mode dependency of the nonlinearity caused by a bolted flange of a simplified model of an aircraft engine casing section. Then, it is proposed to define some criteria explaining this mode dependency and allowing to define which modes could show the most nonlinearities due to the friction joint dynamics. Both experimental and numerical modal testing methodologies will be proposed. It is further proposed to approach the problem from strain analysis, which is quite a novelty in terms of dynamic nonlinearity study. As few studies have been done using this approach so far, a critical point of view will be made regarding the relevance of this method. We should be able to assess whether a strain analysis technique is a good indicator of nonlinearity caused by bolted joints.

(a)

(b)

Figure 1 (a) Combustion Chamber Outer Casing (CCOC) and High Pressure Chamber (HPC) from a Rolls-Royce engine (Left) – (b) CCOC-HPC assembly cut section (Right)

Some nonlinear studies have already been performed on a section of an CCOC-HPC assembly. However, because of the complex geometry of the actual structure, the modal analysis was not easy to correlate with a numerical model. Thus, it will attempt to reproduce a simplified cut section of the CCOC-HOC assembly so that correlations can be easily made between experimental and numerical data. This will be the structure studied in this project. The research methodology has been proposed during the research proposal stage [13]. The methodology presented in the present document has been improved compared to the first proposal. As previously said, both numerical and experimental investigations are performed in this project. This is why, the research methodology is divided into two main axis:

- The numerical model of the structure
- The experimental investigation of the structure

A correlation between the numerical and experimental models is attempted during the whole process. Figure 36 a diagram of the main process of this research project. This aims to give an insight of the global methodology. Each stage will then be further developed in the next chapters.

2 STRUCTURE DESIGN (CAD) AND MANUFACTURING

The aim of the design process was to simplify the CCOC-HOC cut section Figure 1b with the following assumptions:

- The curvature of the casings are assumed negligible
- Thicknesses of left and right parts are constant
- All ribs or equivalent are removed
- There is only the friction plan for the joint positioning (internal cylinder of the right plate removed)
- The compressor radius is considered constant (which leads to a flatness between left and right plate and a constant width for the left plate)

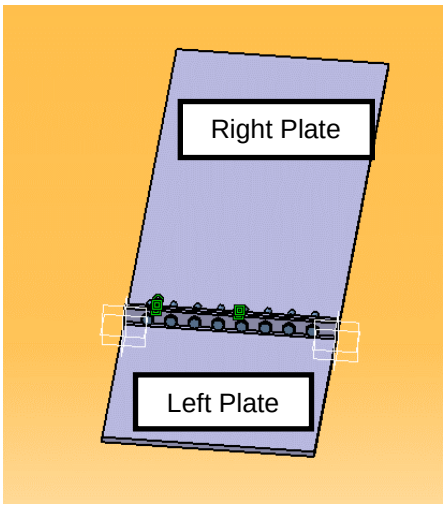

(a)

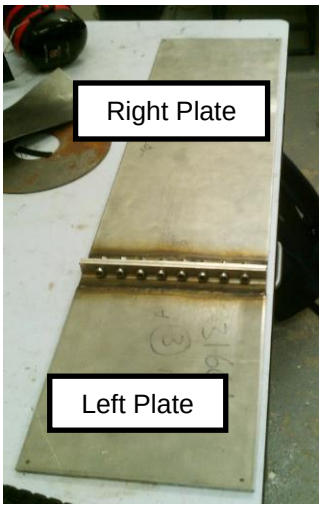

(b)

Figure 2 (a) Left – CAD of the simplified flange structure. (b) Right – Manufactured simplified flange structure

The CAD of the simplified flange structure can be seen in Figure 2(a). The structure needs to be made of stainless steel in order to avoid corrosion that could appear in the vicinity of the joint that could affect its dynamic behaviour. The blank materials have been order to external steel companies. All manufacturing processes have been achieved in the University of Bristol workshops. However, because of the manufacturing capabilities and some process issues that occurred, all the tolerances could not be met.

3 EXPERIMENTAL MODEL VALIDATION- LINEAR CASE

Although the main objective of this project is to study the nonlinear behaviour induced by the bolted joint dynamics, it is essential to start with a linear analysis. It is assumed that the bolted joint does not induce any nonlinear phenomenon if the vibrations levels in the structure are small. From an experimental point of view, that means that the excitation force needs to be relatively small compared to higher levels that could lead to nonlinear responses. From a FEM point of view, the changing parameters from the linear to the nonlinear model are the contact interface characteristics. For the linear model, it is simply assumed that the flanges are “merged”. Thus, there is a linear continuity between the left and the right parts of the structure.

3.1 Modal analysis

The first step of the linear stage is to perform a numerical modal analysis and an experimental modal testing. This has for objective to identify the natural frequencies of the first modes of interest of the structure, with the associated mode shapes. Then, a correlation process will be performed between the experimental and numerical data in order to update the FEM. This updated FEM will be used for further linear and nonlinear analysis. This is one of the reasons why a linear model needs to be performed in a first stage.

3.1.1 Numerical linear finite element model

In the meshing process of the FEM, several types of element types have been investigated. It has been concluded that solid elements need to be used in the case of contact problems. In this case, the structure has been meshed with solid tetrahedral parabolic elements. The mesh size has been optimized so that a good compromise is done between the results accuracy and the calculation time. The meshed structure is shown on Figure 4. It can be noticed that the mesh size is refined in the bolted joint area as this is the area of interest where stress gradients can be important. The nodes belonging to the left and right surfaces in contact are merged.

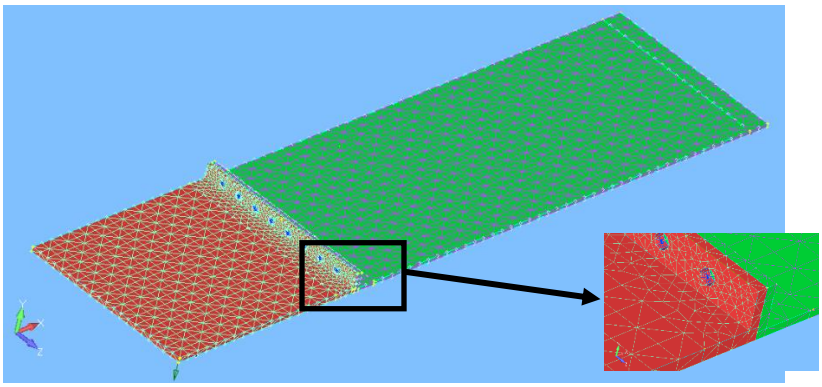

Figure 4 Flange structure mesh (tetrahedral solid parabolic elements)

A modal analysis is performed with a frequency range of 0-500 Hz. This analysis gives the mass normalized modal eigenvectors Φ_n [1] with the associated natural frequencies of the structure. The resulted mode shapes are essential to find the optimized locations of the drive point and sensors that will be set up for the experimental tests. Indeed, the drive point being the excitation location needs to be chosen so that all the modes of interest can be excited. From this first linear modal analysis, we can notice that mode shapes are typical from classic plate structural behaviour, which seems logical regarding the flange structure geometry. This has the advantage simplifying the modal analysis methodology explained in the introduction compared to the complex mode shapes given by the actual CCOC-HPC assembly cut section in Figure 1(b)

3.1.2 Experimental linear modal testing

Modal testing was performed using a Scanning Laser Doppler Vibrometer (SLDV). The flange structure was bolted using nylock nuts that prevent the bolts to get loose under dynamic loadings. A fixed tightening torque (10Nm) was chosen and will remain the same for all the experimental tests. The structure was suspended to achieve free-free conditions. Thanks to the mode shapes predicted by the FEM, test planning could be carried out and the best excitation location identified. It was located at the lower left hand corner of the structure. Figure 5 (a) the SLDV system outside a sound booth in which the test set up was made, as shown in Figure 5 (b).

(a)

(b)

Figure 5 (a) Left – Polytec Laser Vibrometer (LV) – (b) Right – Suspended structure and shaker

The FRFs measured by the laser were post-processed by ICATS modal analysis software [21]. An example of experimental mode shape is shown in Figure 6.

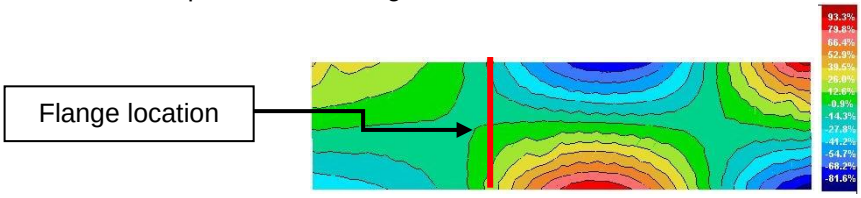

Figure 6 Experimental mode shape of mode 4 (T2) obtained by vibrometry measurements.

3.1.3 Updating process

As both experimental and numerical linear modal analysis were achieved, a correlation can be made between the obtained data in order to update the linear FEM. The mode shapes obtained experimentally using the SLDV measurements are slightly different from those obtained by finite element modal analysis as well as the natural frequencies. Then, a FEM updating process must be performed using the software *FEMtools* [22]. The aim of the updating process is to select some numerical model parameters (in our case the material properties) that will be updated so that the mode shapes and the natural frequencies of the numerical model fit with the experimental results with a limited error. In other words, the mode shapes are scaled once updated. A sketch of the process is presented in Figure 7.

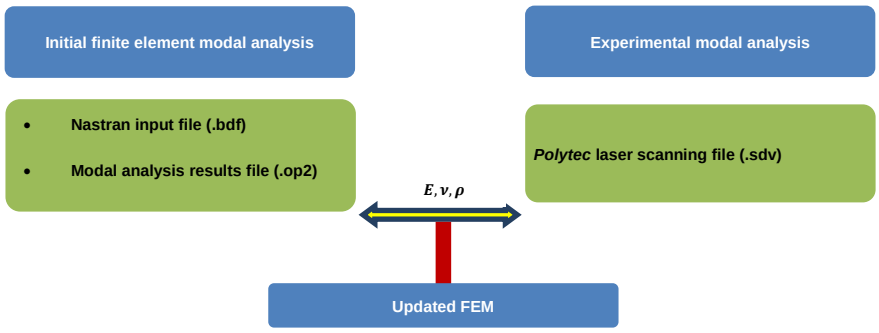

Figure 7 Modal updating process

The first step is to import the experimental test data, which is a group of FRFs (as much as scanning points). Then, a normalized sum of those FRFs is performed in order to extract the poles (at the resonance peaks). The FRFs are then reconstructed to remove the noise from measurements. The Scan geometry needs to be superposed with the appropriate FEM surface. There is then a pairing process of each scanning point to the closest nodes. A first superposition process can be made before the updating process to check whether the FE mode shapes are fine, eventually the updating process can start. Several updating criteria can be chosen. In this presented case, both the natural frequencies and the mode shapes can be correlated by using the Modal Assurance Criterion (MAC) [16]) given as follow:

$$MAC(r,q) = \frac{\left|\{\Phi_{FEM}\}_r^T \{\Phi_{Exp}\}_q\right|}{(\{\Phi_{FEM}\}_r^T \{\Phi_{FEM}\}_r)(\{\Phi_{Exp}\}_q^T \{\Phi_{Exp}\}_q)}$$

Where $\{\Phi_{FEM}\}_r$ is the numerical modal vector of mode r and $\{\Phi_{Exp}\}_q$ is the experimental modal vector of mode q.

The global young modulus E is selected as the only parameter required to be updated. Finally, the correlation function needs to be defined. In this case, it was chosen the CCABS which basically computes the derivative of the response with respect to each parameter and iterates the process by changing the parameters until a given error percentage is reached. Eventually, the initial young modulus that was set to $E = 210000\ Mpa$ has been updated to $E = 204955\ Mpa$. A maximum of 2% of error between the numerical and actual natural frequencies and mode shapes was achived. Figure 8 shows an example of fitted mode shape from numerical and experimental data obtained using the updating process by *FEMtools* [22].

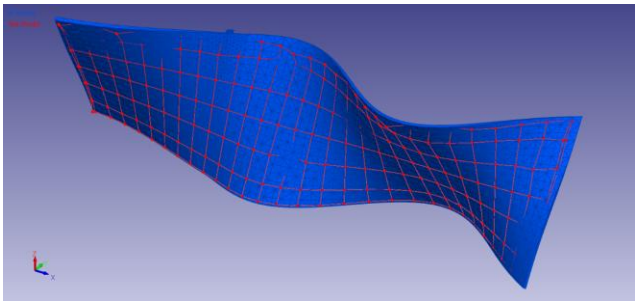

Figure 8 Experimental mode shape (red) fitted with the updated finite element mode shape (blue)

4 NONLINEARITY CRITICALITY MODAL RANKING CRITERIA

As introduced earlier in the paper, the dynamic nonlinearities induced by bolted joints are mode dependent. Then it is important to predict which modes (within a chosen frequency range) will show the most critical behaviour. One of the objectives of this project is to find a way to rank critical nonlinearity based on a linear FE model. An assumption for doing that is to develop some criteria based on a stress analysis using linear modal analysis of the linear FEM. The first stage is to determine the relevant stress components and their location in the vicinity of the joint. R.A. Ibrahim and C.L. Pettit (2003) [3] investigated that the two main physical phenomenon in the bolted joints leading to dynamic nonlinearities are (a) the micro/macroslips occurring in the contact area and (b) localised joint separation that could lead to a “clapping” phenomenon. The friction condition, or the stick/slip limit, can be described in terms of shear stress components within a contact surface area. For example, an infinitesimal cube of a bolted joint contains the two parts in contact and the contact surface area; a simplified stress state can be described as shown in Figure 9. In this case, it is assumed that only the components shown on the figure have an influence on the friction state between the two parts.

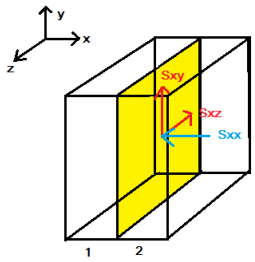

Figure 9 Stress components having an influence on friction between parts 1 and 2, the yellow surface being the contact area.

The total shear stress component of a point in the contact plane is calculated in equation (1)

$$\tau = \sqrt{\sigma_{xy}^2 + \sigma_{xz}^2} \tag{1}$$

The slip condition is reached if

$$\tau > \mu * \sigma_{xx} \tag{2}$$

with μ the friction coefficient, and σ_{xx} the normal component of stress.

In the case of our flange structure, the normal component of stress is mainly given by the surface pressure induced by the bolt preloads. The shear stress is induced by the external dynamic loadings. Then, it is relevant to take $\sigma_{xy}\ and\ \sigma_{xz}$ in the contact plane as references for the stick/slip condition.The separation phenomenon occurs when the normal component of stress goes down to zero at the contact interface. In other terms, it can be described as the sum the normal stress induced by external forces ($\sigma_{xx,ef}$) other than the bolt pressures and the normal stress induced by the bolt pressure ($\sigma_{xx,bp}$). A local separation occurs when $|\sigma_{xx,ef}| > |\sigma_{xx,bp}|$. Then, it is relevant to analyse the normal stresses values obtained in the vicinity of the joint on the lower surface of the plate. Indeed, a separation could only occur close to this surface in the case of this flange structure.

The ranking criteria will be based on cases (a) and (b) separately and a ponderation for each case will be applied. For case (a), the shear stresses $\sigma_{xy}\ and\ \sigma_{xz}$ fields will be analysed in the contact interface plane using the linear FE modal analysis. Although the linear model does not take the bolt preloads into account (since the contact surfaces are assumed merged), this should give an insight of the modal influence on those shear stresses. It is also important to note that modal analysis gives unscaled mode shapes; the absolute values of stress are not relevant also because the interest is to define a rank. For case (b), the normal stress field is analysed along the interface line of the lower surface of the structure. The modal stress results are not presented in this paper**.** Figure 10 shows a table of the shear stresses obtained for mode 6, showing the highest values within the first 10 modes. Figure 11 shows a table of the normal stress obtained for mode 7 showing the highest values within the first 10 modes.

Stress component	Max value (Mpa)	Shear stress field in the contact interface plane
σ_{xz}	49.3	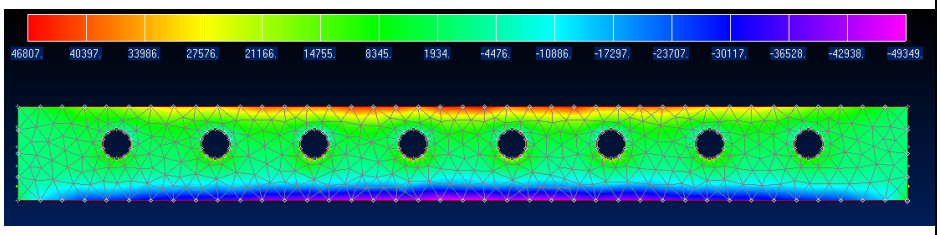
σ_{xy}	20.5	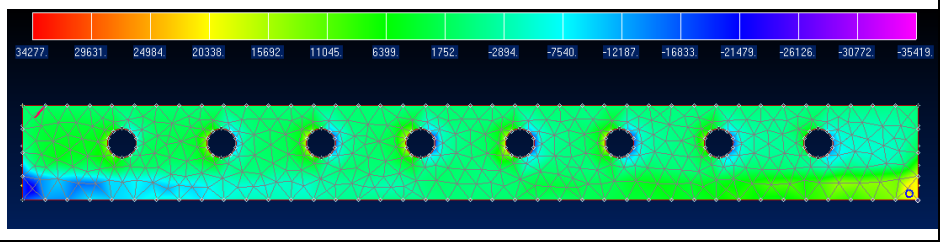

Figure 10 Stress fields for mode 6

Stress component	Max value (Mpa)	Normal stress in the vicinity of the interface line (lower surface of the structure)
σ_{xx}	150.1	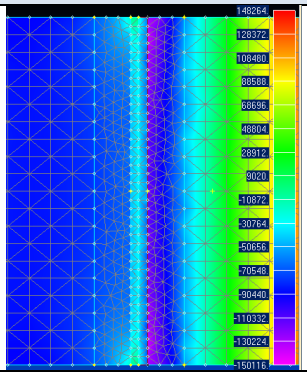

Figure 11 Stress filed for mode 10

It is obvious that the maximum value of stress itself does not have a relevant meaning. The surface area of high stress has also been taken into account. In this analysis, we could notice that the bending modes show the highest values for the separation criteria (case (b)). The torsional modes show the highest shear stress values which seem logical. Then, they are the most likely to show microslip phenomenon (case (a)). Finally, assuming that the case (a) is twice more critical as case (b), after applying this ponderation (physical assumption), we obtained the final nonlinear criticality ranking below (1 being the most critical), as presented in Table 1.

Ranking	Mode	Type
1	6	T3
2	8	T4
3	7	B4
4	4	T2
5	5	B3
6	2	T1
7	3	B2

8	9	
9	1	B1

Table 1 Ranking of modes based on stress criteria

Note that the modes studied are slightly different from the ones obtained with the updated FEM. Then, mode B5 (normally mode 9) does not appear here. However, we will attempt to validate this prediction ranking with 3xperimental data for the most critical ones (T3, T4, B4, T2).

5 NONLINEAR MODAL TESTING OF THE FLANGE STRUCTURE

This section will present an attempt to validate the nonlinearity criticality ranking modal testing methods [1]. In many vibration nonlinearity researches presented in the literature review [2], the nonlinearity is usually identified using the Frequency Response Function (FRF) of the structure within a relevant frequency range and the appropriate experimental set up. In those studies, a single mode is generally selected and several FRFs are generated around its natural frequency for several level of forcing input. Then, if the friction joint induces nonlinearities, they can be highlighted when the different FRFs are not superposed. For example, Eric Chatelet and his colleagues [13] have shown this effect using a single degrees of freedom (SDOF) friction joint structure. For a fixed normal force applied on the assembled parts, they generated several FRFs for increasing levels of tangential forcing. The receptance (displacement response divided by the input force) first decreases because of increasing damping due to microslip. Then, the joint becomes loose (macroslip) and the receptance increases again. There is also an important frequency shift to the left induced by a decreasing joint stiffness. In our case, we will attempt to generate those FRFs for every mode of interest. Then, we will be able to identify the modal nonlinearities through specific post-processing methods described further in this part. Finally, the most critical modes will be compared to the prediction ranking established using the linear FE modal analysis.

5.1 Experimental set up

As previously said, the main objective is to generate some FRFs for each mode for several levels of excitation. This modal testing process will be carried out for a single force input point and a single output response point. Those two points have been set using the FE linear modal analysis. The output response location needs to be close to the flange if we want to capture the nonlinearities (which are mainly localised around the joint). The structure itself is suspended vertically in the same way as for the linear modal testing. The excitation direction is set to be horizontal (perpendicular to the flange structure's main plane), in order to limit the effect of pre-stress cause by the inertia of the structure. The global experimental set up is illustrated in Figure 9.

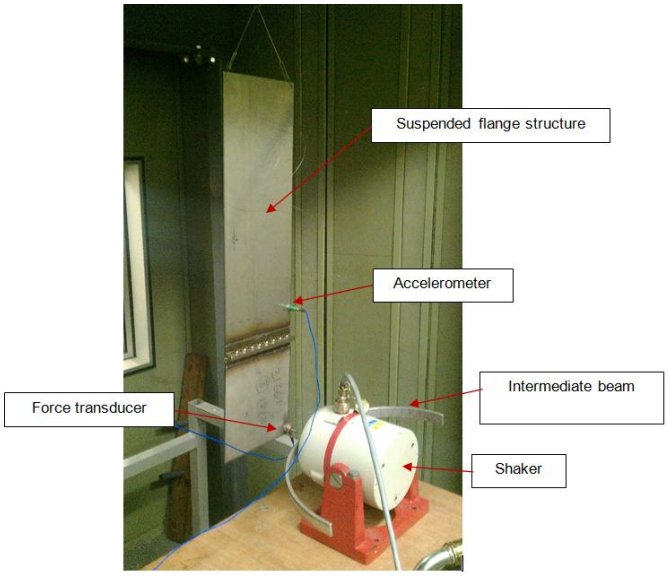

Figure 12 Experimental setup

The structure is excited using a horizontal shaker (*LDS v406*). This shaker is controlled by the *LMS* acquisition module (*LMS SCADAS III*) via an intermediate amplifier (*LDS PA25E*). A force transducer (*PCB 208 C03*) is placed between the shaker tip and the excitation point on the structure's upper surface. The output response is captured by an accelerometer (*PCB 333M07*) glued over the flange on the upper surface. The *LMS* acquisition is fitted with a signal processing software which is able to perform signal control. The measurements are performed with three types of control:

- **Without control**: the output signal voltage is fixed. The advantage of this technique is its execution rapidity. It is convenient to quickly scan a large frequency range and generate a FRF. However, it is not relevant when it comes to comparing the FRFs for different levels of vibration, since both force and acceleration can vary all along the scan.
- **Acceleration control** (or amplitude control): the response output is controlled. Then, the force varies around the natural frequency. Approaching the natural frequency peak, the force decreases while the acceleration amplitude remains constant.
- **Force control**: the force input level is controlled. Then, the output response varies while the force amplitude remains constant. The acceleration increases when approaching the frequency peak. This is the most usual type of FRF generation process.

It can be seen in Figure 12 that an intermediate beam is added between the shaker and the structure. It aims to create more impedance at the excitation location. The beam was not tuned for all modes but for some particular resonances, the beam resonated and thus reducing the energy required by the shaker to excite the structure.

5.2 Modal testing

5.2.1 Modal testing without control

The first stage of the modal testing consists in scanning the whole frequency range of interest with low excitation amplitude (linear coupling conditions). A frequency range of 0-600 Hz was defined for a low excitation force and the resonances of the test structure were identified. Three levels of output signal were chosen corresponding to Low, Medium and High; this was done in order to identify response peak distortion due to nonlinearities. After reduced frequency ranges were defined for each mode, and then it was possible to test those separately with three levels of excitation. Unfortunately, the results were not satisfying without control, since the chosen levels were not high enough to observe any nonlinearity.

5.2.1.1 Modal testing with force control

The next step has been to perform the FRF measurements with force control. Then, it is a more relevant control type to compare the different modes to each other with different levels of forcing. However, although it seems to be the best FRF measurement technique, it is also the most difficult to control for the *LMS* controller. Indeed, when approaching a natural frequency, the shaker amplifier struggles to deliver enough power to maintain a given level of forcing. Those measurements have been performed for three levels of force amplitude: 0.5, 1 and 2 N. Again, it has been noticed that for most of the tested modes, those amplitudes were not high enough to induce any significant nonlinearities. Besides, the experimental FRFs were too noisy because of the control difficulty encountered.

5.2.1.2 Modal testing with acceleration response control

This last measurement stage has been the most successful to generate FRFs showing the nonlinearities induced by the flange bolted joint. Here, this is the output response which is controlled (in our case as an acceleration). In order to compare the tested modes to each other, it has been attempted to set similar acceleration amplitudes for every modes. However, this has not been possible for some modes which observability was low compared to others. For example, as we previously said, mode 5 shows a low observability and the maximum output response (acceleration) which could be achieved was very low compared to the average maximum of every other mode. We were also sometimes limited by the amplifier capacity to achieve high levels of vibrations (which could have induced more nonlinear behaviour).

5.2.1.3 Measurement process

The measurement process was:

- Define a reduced frequency range for each mode of interest.
- Define the sweep frequency step: 0.05 Hz in our case. Indeed, it has to be small enough to capture enough data points around the natural frequency peak, but not too small so that the sweep time of a mode is not too long.
- Define the controlled acceleration level for each FRF generation.
- Repeat the frequency sweep for several levels of acceleration up to the maximum amplifier capacity or control limits.

The overall measurement process has been rather long. Indeed, although this modal testing process seems trivial, there are many external factors that are likely to lead to measurements issues. For instance, the way the structure is suspended, the shaker tip is positioned and attached are two sources of measurement dispersion.

5.2.1.4 Data post-processing

Most of the modes of interest in this study show some nonlinearities, the advantage of performing the measurements with acceleration control is that most individual FRFs generated are linearized and can be analysed using linear modal analysis tools. In the case of force control, a complex nonlinear post-processig is often required as the FRFs generated can be highly distorted for high levels of force. This is why, for the convenience of measurements and data post-processing, the nonlinearity identification is performed using the amplitude control technique.

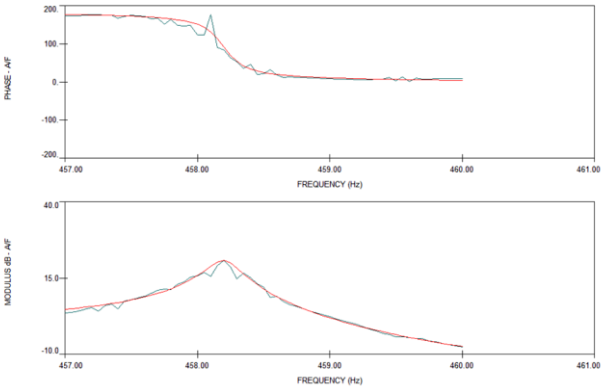

Figure 13 FRF curve fitting process in ICATS for mode 10 (the green curve being the experimental data and the red one being the regenerated linearized FRF)

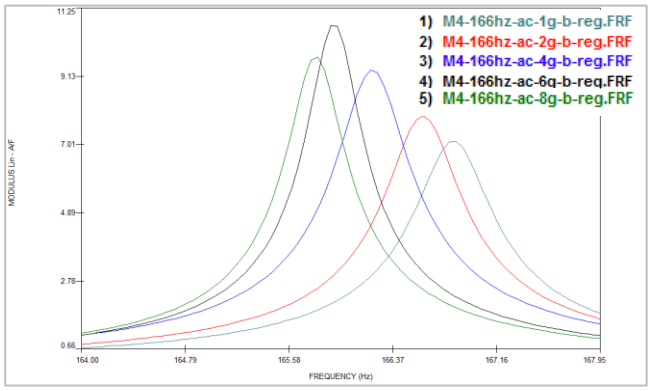

Figure 14 Linearized FRFs for modes 4

Another nonlinearity indicator is the normalized modal damping coefficient defined as the ratio of the modal damping coefficient of the linearized FRF of a given level of vibration by the one of the lowest level of vibrations. Figure 15 shows the results of this type of analysis.

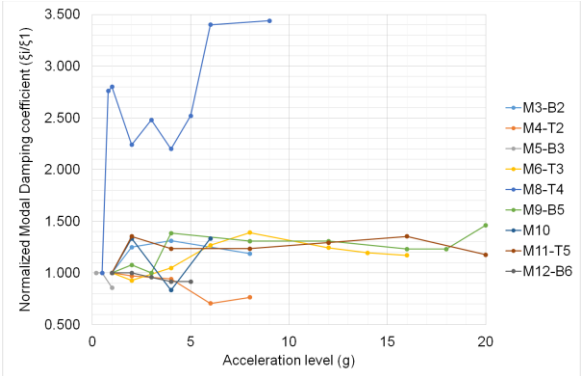

Figure 15 Evolution of the Normalized Modal Damping as a function of the acceleration level (g)

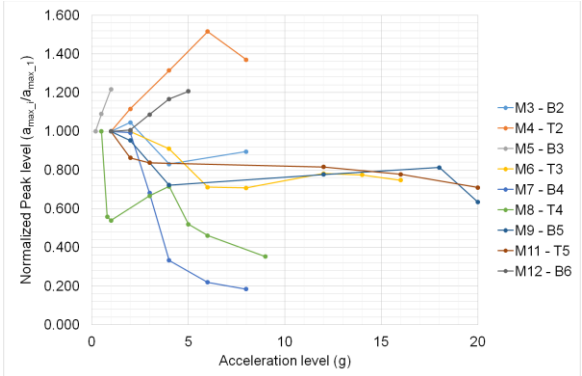

Figure 16 Evolution of the Normalized Modal FRF peak levels as a function of the acceleration level (g)

This graph, in Figure 15, does not give relevant nonlinear information as we expected. Indeed, the modal damping is supposed to be a parameter affected by a nonlinearity induced by a friction joint. Only mode 8 shows an important increase in modal damping although most other modes also show a slight increase in damping. However, it can be noticed that mode 4 shows a decrease in modal damping, which was not expected but can be explained as seen further. This is partly due to the curve fitting process performed using *ICATS*, where the damping coefficient is sensitive to the fitting quality. Then, it has been decided to study the evolution of peak level instead of modal damping coefficient, although those parameters are similar. The normalized peak evolution seems to be a more relevant nonlinearity indicator in the case of our flange structure. Indeed, the modes showing a nonlinear trend can be observed here. Modes M6, M7 and M8 show a clear decrease in peak level with increasing vibration amplitude. On the other hand, modes M12 and M4 show an increase in peak level which will be further explained. Finally, the last nonlinearity indicator is the normalized Natural Frequency (NF) evolution of each linearized FRF. Indeed, a nonlinearity caused by a bolted joint is often associated with a shift in frequency due to a decrease in joint stiffness with an increasing level of vibrations (as it has been explained in the literature review [2]). However, the actual change is frequency was rather small and data are not reported in this paper. The NF shift can be clearly observed here for mode M4, M6 and M8, although its normalized value is relatively low (less than 1% in the tested frequency range).

From all those nonlinear indicators analysis, an actual nonlinear criticality ranking can be established and compared with the prediction. However, only the four most critical modes will be retained as the other modes (the least nonlinear) are not easy to compare with the data acquired. It is important to note that all modes could not be tested properly for several reasons previously explained. However, from the measurements done on similar structures [6], those four most critical modes seem relevant.

FEM prediction ranking	Experimental Ranking	Mode	Type
2	1	8	T4
3	2	7	B4
4	3	4	T2
1	4	6	T3

Table 2 Simulated and experimental ranking of nonlinear modes

Mode 7 (B4) data was probably wrong. Indeed, a “jump” phenomena appears on the high vibration level FRFs that probably comes from a control issue. Then, it has been inserted in the most nonlinear modes with caution. Some further measurements would have been necessary for this mode. Although the ranking was not exactly similar using the FEM prediction criteria, those four most critical modes were captured. This means that the criticality ranking criteria can be partially validated. It is not an accurate technique but allows to identify the modes likely to show the most nonlinear behaviour. Another conclusion to this experimental analysis is the nature of nonlinearity that can be different for every mode. The influence of the bolted joint dynamics on the structure behaviour varies from a mode to another. That confirms the assumption that the nonlinearities induced by friction joints are mode dependant. For instance, mode 4 (T2) shows an increase in accelerance peak level with an increasing vibration level, whereas mode 8 (T4) shows the opposite. The type of nonlinear behaviour shown by the former mode has been widely observed in bolted structure dynamics [2]. The nonlinear behaviour of mode 4 (similar to some bending modes) could be assimilated to the analytical case of a cracked beam. Indeed, Wagg, D.J. & Neild S.A. [17] developed a simplified analytical model of a cracked beam that allows to generate the backbone curve of its first bending mode using the Harmonic Balance Method (HBM). The backbone curve is a useful tool in the case of nonlinear vibrations. It defines the undamped natural frequency as a function of the response of the system when no damping or forcing is present. The peak of each resonance curve crosses this backbone curve. When a backbone curve shows a decreasing natural frequency for an increasing structure response, it expresses a softening effect. Indeed, in the case of a cracked beam, when the surface containing the crack is in bending tension, it opens and the local stiffness decreases. In opposition, when this surface is in compression, the crack closes and the local stiffness is higher. This could also be the case for the flange structure. The joint at the lower surface of the structure can be assimilated to a crack. In part II, it has been seen that the highest normal stresses are in this area, especially for bending modes.

6 NONLINEAR DYNAMIC INVESTIGATION USING STRAIN ANALYSIS

So far, the nonlinear analysis has been performed using classic modal testing tools, that is to say, mainly based on FRFs generated using a single output response. Most nonlinear vibration analysis are based on those methods. As we have seen before, the vibration nonlinearity induced by friction joints is mode dependant as the stress field in the vicinity of the joint is specific to each mode. From the linear FE modal analysis, an assumption has been made that the torsional modes are the most likely to show microslip behaviour in the contact interface as the shear stress is important as well as its surface area. The bending modes are more likely to show a joint separation behaviour as the normal stress along the joint line is more important than torsional modes. Those assumptions need to be validated by experimental data as well as further numerical analysis based on strain/stress outputs instead of acceleration in a single point.

6.1 Experimental strain measurements

6.2 Strain gages setup

It has been seen in section 4 that the critical stress, likely to lead to nonlinear behaviours, are located both at the contact interface (especially the shear stress components) and on the bottom surface of the structure along the joint line for the normal stress components. However, the contact interface strain/stress components are not measurable with the common strain measurement techniques. Strain gauges were planned at locations on the casing of the test structure and in order to keep the generation data sensible four points were selected. Two measurement points were selected at the edge and two at the middle of the test structure. Each pair were displaced to be one on the short and one on the long flange, as shown in Figure 17. This layout was planned to capture possible changes across the flange for an excitation given at the shorter component.

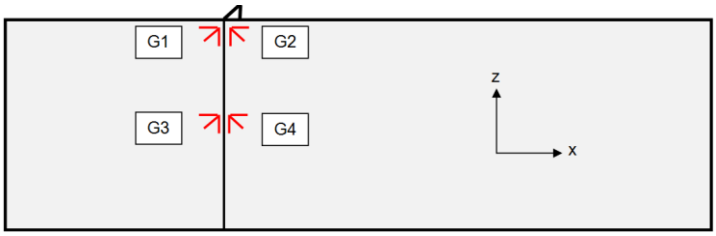

Figure 17 Measurement points for the strain gauges

It was possible to measure σ_{xx}, σ_{zz} and σ_{xz} (plane stress). However, for the case of interest, σ_{xx}, which could induce a partial separation of the bolted joint, and σ_{xz} , which was related to the friction behaviour of the bolted joint (even though it is not located at the joint interface, it could give a good insight), were relevant to the test. Now, in terms of strain components (the measurable quantity), the Hooke strain-stress relationship for plane stress gives:

$$\sigma_{xx} = \frac{E}{1-\nu^2}(\epsilon_{xx} + \nu\epsilon_{zz}) \quad (3)$$

$$\sigma_{xz} = \frac{E}{1-\nu^2}(1-\nu)\epsilon_{xy} \quad (4)$$

Then, $\epsilon_{xx}, \epsilon_{zz}$ and ϵ_{xz} are required to get the stress components of interest. This is possible to measure those strain components with three components gages or so called rosettes [18]. The 45° rosettes gages were carefully attached on the casing surface, as shown in Figure 18. This has been done with a particular attention as those are very sensitive sensors. It is clear from Figure 18 that many cables are not connected to the gauges and these are seen as possible source of damping in the system.

(a) (b)

Figure 18 Flange structure equipped with four rosette gages

6.2.1 Experimental process

One of the main objectives of this investigation is to capture some information based on strain data that could reveal and identify nonlinear behaviours due to the bolted joint dynamics. As a first experimental campaign has already been carried out using the classic modal testing methods, we will attempt to use some of its experimental setup parameters in this investigation based on strain analysis. The proposed experimental method is to capture the strain components of interest (for every gages) for the first 12 modes with a low, medium and high vibration levels, see for example mode 4 (T2) in Figure 19. In order to remain consistent with the previous nonlinear FRFs measurements, the structure is excited in the same configuration (suspended in its vertical position) as it can be seen in Figure 20. Single tone excitation measurement was executed for every controlled level of vibration. For each modes, three measurements are performed using a low, medium and high acceleration amplitude (at the accelerometer position) determined using the nonlinear FRFs previously acquired. For each level, the nonlinear natural frequency is chosen.

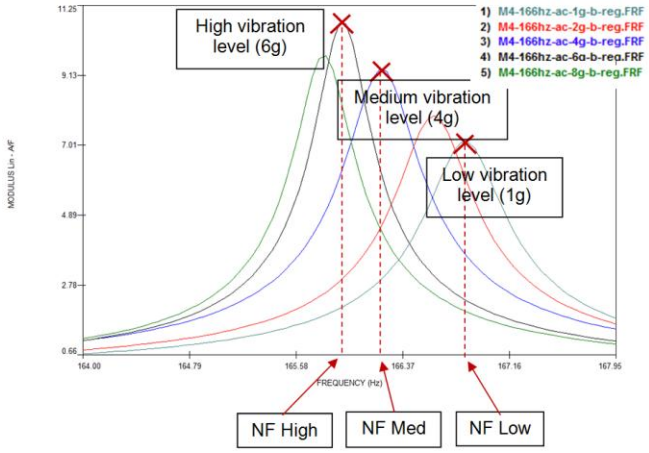

Figure 19 Example of FRF for mode 4 (T2)

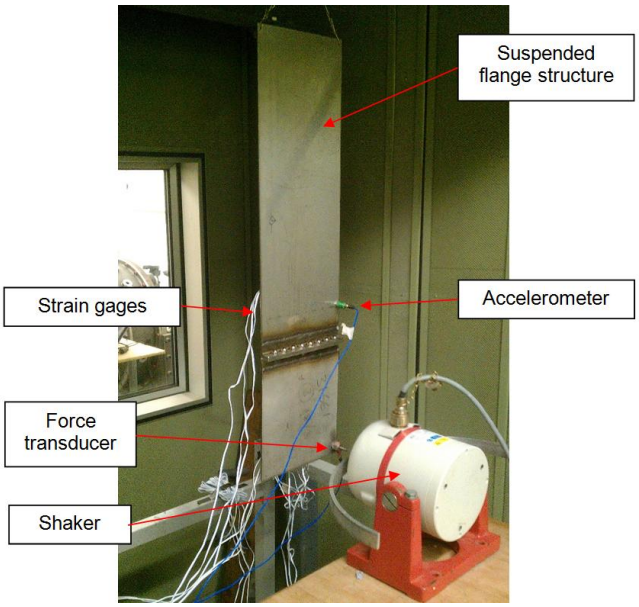

Figure 20 Test setup with strain gauges

The force, acceleration and strain data are acquired via a *National Instrument* acquisition card. It is then processed with a *LabView* software specifically created for this purpose. Below is a diagram of the whole acquisition chain used for this strain measurement campaign.

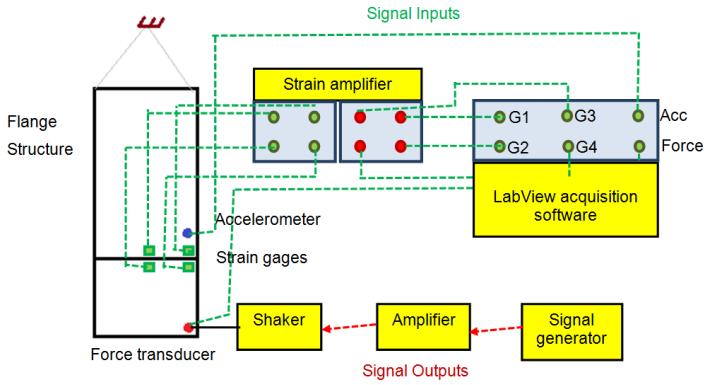

Figure 21 Acquisition setup

The *LabView* acquisition software is designed in such a way to acquire both the acceleration from the accelerometer, the force from the force transducer and the twelve strain components from the strain gages. Once the desired acceleration or force level is reached by manually changing the shaker amplifier gain, and the natural frequency is set, all those input data are recorded during 10 s (steady state response). This acquisition time is chosen so that the Fast Fourier Transformation (FFT) of the signals done during the post-process.

Most values of strain amplitudes obtained during those measurements are very low (between 1 and 100 $\mu\epsilon$). As a result, most strain signals are very noisy. This can be explained by the natural noise delivered by the strain gages relatively high. In some cases, the ratio Signal/Noise was inferior to 5. Then, it was necessary to post-process the signal in order to retain only the useful information from the data acquired. For linear conditions, the strain signals are supposed to be sine waves like the force and acceleration. But this was not the case because of this noise issue. For example, Figure 22 shows a portion of the time domain signal acquired of the normal strain captured by G1 for mode 6 ($f = 270\ Hz$) for a level of excitation of 2g (linear conditions). Many high frequency components can be seen, most of them are due to the gage noise.

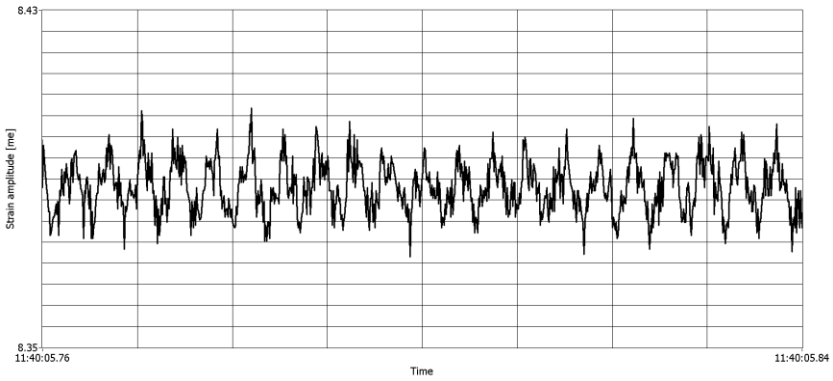

Figure 22 Time domain signal of ϵ_{xx} of G1 for mode 6 (T3) at a level of vibration of 2g

6.3 Signal post-processing

Nonlinearities manifest by a number of additional spectral components multiple of the fundamental one, which is the response to a single tone excitation waveform. These harmonics can be observed in the acceleration, velocity or displacement output but this should also be observed in the strain signals Therefore a spectral analysis of the strain signal is performed.

6.3.1 Notations

As many strain components, gages, levels of vibrations and harmonic orders are used in this analysis, a notation has been chosen containing all information:

$$G_k \epsilon^{i}_{xx\_H_j} \quad (5)$$

Where the following subscripts mean:

- i: level of vibration (1, 2 or 3 for Low, Medium or High)
- k: Gage number (1, 2, 3 or 4)
- xx: Strain component ($xx, zz\ or\ xz$)
- j: Harmonic order (1, 2 or 3)

For example:

$$G_1 \epsilon^{3}_{xx\_H_2}$$

is the second harmonic amplitude of the normal strain given by gage 1 for a high level of vibrations.

6.3.2 Post-processing objectives

As it has been previously said, the main objective of this study is to assess the relevance of strain analysis for highlighting the effect of dynamic nonlinearities caused by bolted joints. It was realized that being the values of strains very low their absolute values were not considered important. Indeed, this nonlinear experimental investigation is not suited for establishing a nonlinear criticality ranking based on absolute values of strain amplitudes. Instead, below is a listing of analysis suggestions that have been performed to study the impact of joint nonlinearities on strain:

- Is there a discontinuity in some strain components fundamentals between two facing gages when the level of vibration increases?
- Is there a discontinuity in some strain components harmonics between two facing gages when the level of vibration increases?
- Does the strain data give more information about harmonics caused by dynamic nonlinearities than the acceleration output signal?

In order to answer those problems, a post-processing program using *LabView* is created. It allows to perform the spectral analysis of every measured signals (acceleration, force and strain components) and gives the amplitudes of the fundamental (H1), the second harmonic (H2) and the third harmonic (H3).

The amplitudes of fundamentals and harmonics need to be normalized between the three levels of vibrations. Two different normalization methods are used:

- (a) Normalization of all values with respect to the value obtained for the low level of vibration (for both acceleration, force and strain components):

$$Normalized\ value\ (a) = \frac{G_k \epsilon^{i}_{xx\_H_j}}{G_k \epsilon^{1}_{xx\_H_j}} \quad (6)$$

- (b) Normalization of the second and third harmonics (H2 and H3) with respect to the fundamental amplitude (for both acceleration, force and strain components):

$$Normalized\ value\ (b) = \frac{G_k \epsilon^{i}_{xx\_H_j}}{G_k \epsilon^{i}_{xx\_H_1}} \quad (7)$$

Then, the first type of normalization should allow to observe any kind of nonlinearity from a low to high vibration level. For a linear behaviour, every curve (normalized values as a function of the vibration level) should be linear. If a curve shows something different than a line, it could come from nonlinearities caused by the joint. However, it was discovered that the harmonic values can be close to zero in linear conditions. Then, this normalization method is not relevant anymore since it relies on the absolute values obtained for a low level of vibration. This is why, the second type of normalization seems to be more relevant to show any discontinuity. For more convenience, the normalized value is given in percentages. If no nonlinearity appears, there should not be any harmonic, giving a normalized value of 0%. However, it only shows information about the second and third harmonic values. This is why a combination of two normalization methods is proposed in this nonlinear analysis.

6.4 Strain results analysis

Strain data is analysed by generating some graphs representing the normalized values of acceleration, force and strain components as a function of the level of acceleration (low, medium and high). For each mode, a separated graph is generated for every gauge association (1 and 2 or 3 and 4) and for every output result type (acceleration, force, normal strain and shear strain). And this is done for the two types of normalization previously explained. Modes 4, and 8 are presented in this paper. The first type of normalization previously explained is identified with an index (a) while the second type is represented by the index (b).

6.4.1 Mode 4 (T2) – 166 Hz

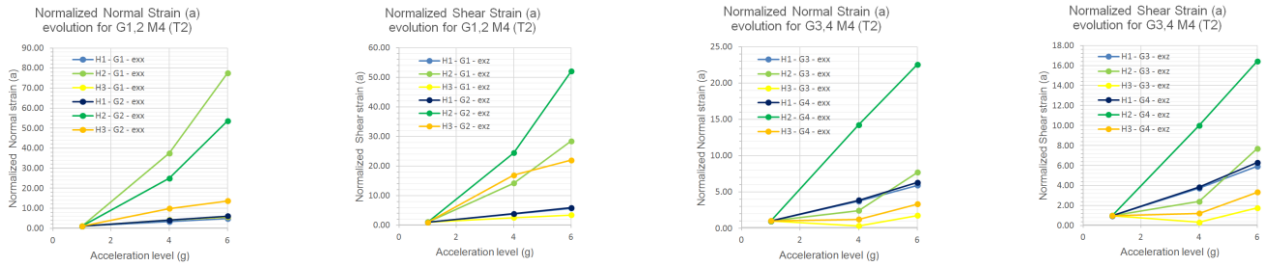

Figure 23 Evolution of the normalized (a) values of normal and shear strain for gages 1,2,3 and 4 as a function of the acceleration level (g) for mode M4 (T2)

A perfect linear behaviour would show horizontal lines for the harmonics (as they would theoretically be zero) and two superposed linear curves for the fundamentals. In this case, the same trends are observed for both the normal and shear strain. The fundamental curves (H1) are almost superposed in every case. That means, no discontinuity is observed from the fundamental level. However, the second harmonics get large from the medium level of forcing. In terms of discontinuities, the normalized values for the second and third harmonics are higher for gauges 2 and 4. That could show a discontinuity between the left and right plate, with more strain nonlinearities at the right plate. The graphs presented Figure 25 show the strain data for gauges 3 and 4 (middle of the plate).

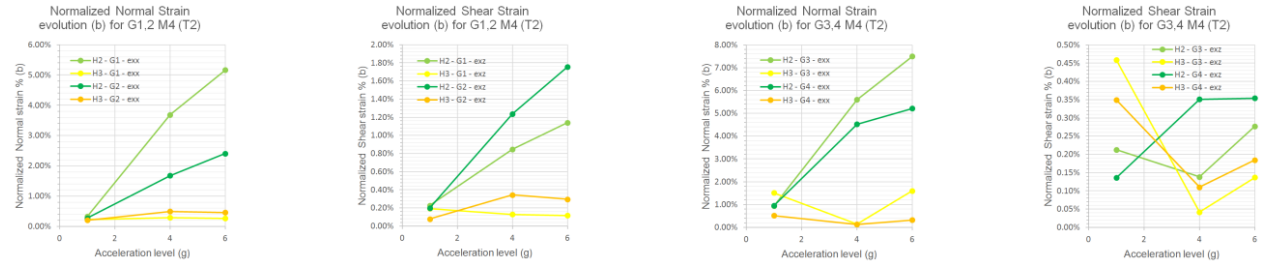

Figure 24 Evolution of the normalized (b) values of normal and shear strain for gages 1,2,3 and 4 as a function of the acceleration level (g) for mode M4 (T2)

The first feature observed is the increase in second harmonics with an increasing level of vibrations, which indicates that this mode shows a nonlinear behaviour. It can be seen here that the normalized values of harmonics are more significant for the normal strains (up to 7% of the fundamental) from the medium level of vibration. This is only the case for the second harmonic though since the normalized H3 are always below 1%. Besides, discontinuities are observed between the left and the right plate in the second harmonic of normal and shear strain. In the case of normal strain though, the left plate shows more important H2 values.

6.4.2 Mode 8 (T4) – 359 Hz

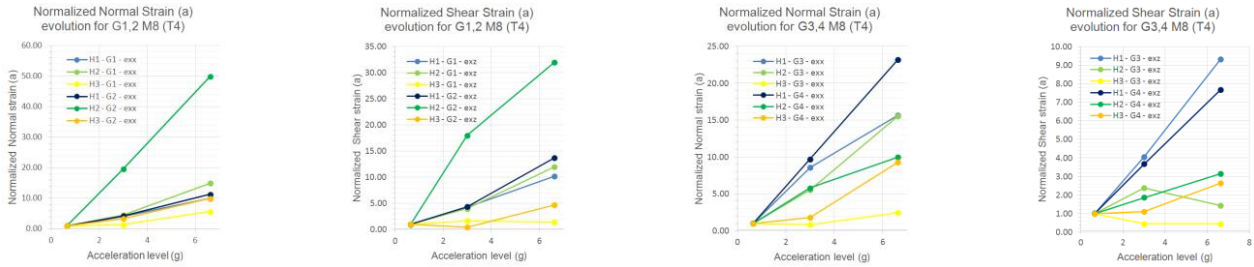

Figure 25 Evolution of the normalized (a) values of normal and shear strain for gages 1,2,3 and 4 as a function of the acceleration level (g) for mode M8 (T4)

For gage 1 and 2, $G_2\epsilon^3_{xx\_H_2} > G_1\epsilon^3_{xx\_H_2}$ and $G_2\epsilon^3_{xz\_H_2} > G_1\epsilon^3_{xz\_H_2}$. This could be due to a discontinuity (higher nonlinearity on the right plate). For gauges 3 and 4, discontinuities can be observed for H1, H2 and H3 for the high level of vibrations, especially for the normal strains.

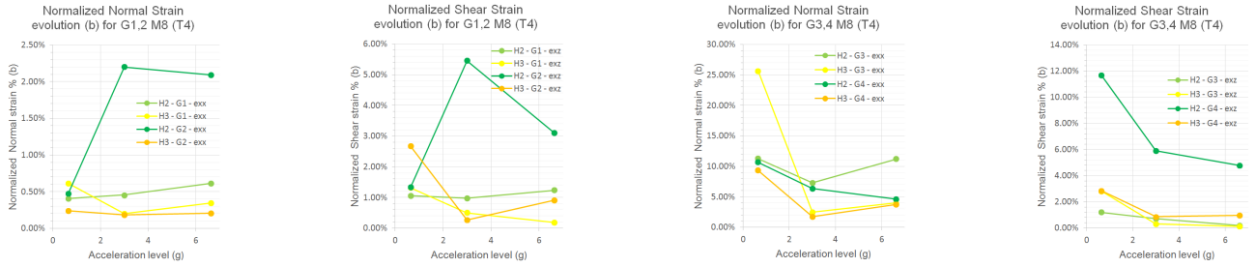

Figure 26 Evolution of the normalized (b) values of normal and shear strain for gages 1,2,3 and 4 as a function of the acceleration level (g) for mode M8 (T4)

For gage 2, a high relative second harmonic is observed from the medium level of forcing (for both normal and shear strain), showing a high nonlinearity. Moreover, this nonlinearity seems to be localised on the right plate since $G_2\epsilon^{2,3}_{xx\_H_2} > G_1\epsilon^{2,3}_{xx\_H_2}$ and $G_2\epsilon^{2,3}_{xz\_H_2} > G_1\epsilon^{2,3}_{xz\_H_2}$. However, no conclusion can be made from the strain measurements of gages 3 and 4.

The force and acceleration graphs are not presented in this present document as they would add too much data. However, a similar trend has been observed for every mode presented above. The acceleration harmonics normalization of type (b) usually follows the same trend as $G_2\epsilon^2_{xx\_H_2}$. This seems reasonable as both values are measured on the same plate and are rather close (less than 50 mm). However, the normalized values are generally higher for the strain data than the acceleration, which shows the relevance of using the strain data as a nonlinear indicator instead of acceleration. From this nonlinear strain experimental investigation, several conclusions can be made to assess this nonlinearities identification method:

- For every modes showing the highest nonlinearities identified using classic modal testing methods, some nonlinear patterns have been confirmed using strain analysis.
- One of the advantage of strain analysis over classic modal testing is the ability to capture some local nonlinearities due to the joint. For instance, some discontinuities have been shown between the left and the right plate, highlighting the influence of the bolted joint on the structure. Besides, different nonlinear features were observed between the (1,2) and (3,4) gage couples, highlighting the localised nature of nonlinearities induced by the bolted joint.
- Another advantage of strain measurements is that the sensors (strain gages) have a lower influence on the structure behaviour as accelerometers could have (in terms of added mass). However, the gage cables could have added a slight damping to the structure.
- However, in opposition to the classic modal testing method, no defined way to quantify the nonlinearities has been clearly found so far. Two normalization methods have been proposed which do not show the same nonlinear features, although the second one (b) seems to be the most relevant.

- Another disadvantage of strain measurements is that the absolute values can be very low and even close to the level of noise generated by the strain gages. This can induce some odd results as it has been observed for modes 7 and 8. Indeed, if the fundamental value of a strain component is low, it becomes uncertain to study the evolution of its relative harmonics as a function of the vibration level.
- Finally, we are also limited by the locations where the gages can be glued on the structure. In the case of friction joints, special strain measurement have to be used to know the strain field within the contact interface (still not well known nowadays). However, the FEM could be used to correlate those values of strain if the values of strain are known in another region of the structure.

7 LINEAR CORRELATION FOR MODEL VALIDATION

A linear strain investigation has also been performed in order to compare the normal and shear strains of each mode and to validate the FEM with strain outputs.

7.1 Linear FRF correlation

The strain components of the numerical model are generated using a frequency response function based on the linear modal analysis. In this type of numerical analysis, a structural damping [1] can be added to the solver. This parameter has an important impact on the response level of the structure subjected to a harmonic excitation. After several trials and errors, an optimized value of structural damping is set to 0.5 %. However, the value chosen did not produce perfect correlation between simulated and measured response. This would be reflected on the strain values calculated and therefore it was decided to use trends of strains of components and compare those between the numerical and experimental linear analysis.

7.2 Linear modal strains correlation

The numerical FRF analysis requires a fixed periodic input (a force in our case). This suggested that the excitation force level is controlled in both numerical and experimental linear tests. From the previous experimental measurements, a forcing value giving quasi-linear conditions is set to 0.4 N. Then, the normal and shear strain components are measured at each natural frequency of the first ten modes for both experimental and numerical linear analysis. The graphs, in Figure 27 and Figure 28, present the linear strain results obtained experimentally and with the linear FEM for the strain gages positions presented in Figure 18. It can be observed that the normal strains are well correlated between the measurements and the model whereas some differences are noticed for the shear strain component. This is can be explained by several reasons. The errors can come from the uncertainties in the measurements in the way the shear strain has been computed from the rosette components and the fact that the values are close to the natural noise level of the strain gages. This could also come from the numerical model as the output points chosen are not exactly at the actual gage position. Besides, the mesh is probably not fine enough to capture accurate values of strain since the gradient can be rather high around the bolted joint. The normal strain amplitudes are always higher for gages located on the right plate. This can be explained by the difference in thickness between the left and right plate. It is thinner on the right plate, giving higher normal strain values. This is not the case for the shear strain though. Moreover, as expected, the shear strain amplitudes are higher for the torsional modes (especially modes 2, 4 and 6). However, there is an unexplained ten factor between the experimental and numerical values. This is why we will not pay attention to the absolute values of strain in the next part.

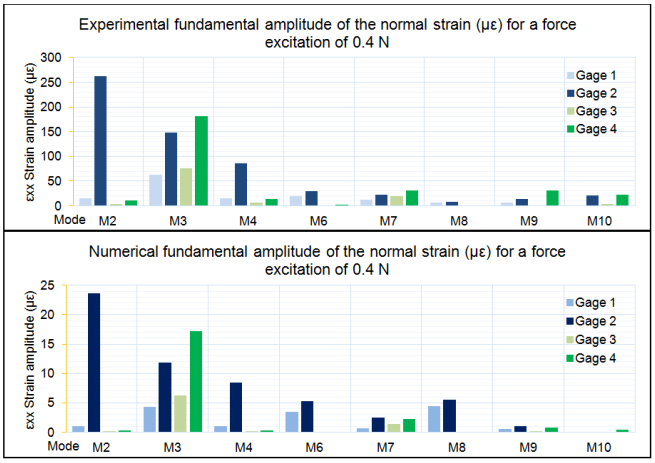

Figure 27 Experimental and numerical fundamental amplitudes of normal strain (με) for a harmonic force excitation of 0.4 N

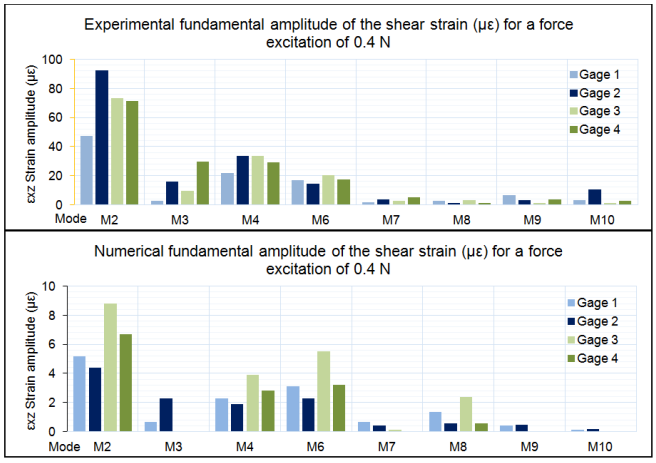

Figure 28 Experimental and numerical fundamental amplitudes of shear strain (με) for a harmonic force excitation of 0.4 N

7.3 Numerical time domain nonlinear analysis

As the linear FEM has been validated, a nonlinear analysis can be performed and compared with the experimental results. These analyses will be performed in the time domain. Indeed, it would also have been interesting to generated nonlinear FRFs to be compared with the experimental results. However, in finite element analysis, this generally induces a complex process combining the Multi-Harmonic Balance Method (MHBM) and an alternating frequency time method as it has been seen during the ASME Turbo Expo [12] in the paper written by A. Herzog, M. Krack, L. Scheidt and J. Wallascheck [19]. This numerical process involves additional software not available in this study. Several time-domain nonlinear analyses are performed for the most critical modes (M4 and M8) using low and high excitation forcing levels. The objective is to compute the time response of the flange structure in terms of acceleration and strain for the natural frequencies of modes 4 (T2) and 8 (T4). The structure is subjected to a harmonic force input with low and high amplitude.

7.3.1 Nonlinear model parameters

7.3.1.1 Joint interface modelling

In Finite Element Analysis, there are several ways to model friction joints. Most of them have been presented in the Literature Review [2]. For bolted joints, the most common process consists in modelling the bolts with rigid elements. These are elements that connect two nodes in a rigid way, one being the “master”, the other the “slave” (the displacement of the slave only depends on the master’s one). A first model has been created using rigid elements for the bolts and shell elements for the rest of the structure [14]. Part of the bolted joint of the flange structure model can be seen in Figure 29.

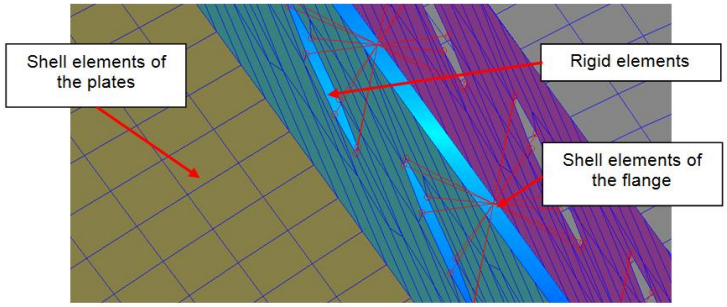

Figure 29 Finite Element Model of the flange structure using rigid elements for the bolts and shell elements for the plates and flange

This has the advantage of being a linear and simple model (leading to a relatively short computational time). It is able to give a first insight of the linear mode shapes and associated natural frequencies. However, it does not capture any nonlinear behaviour induced by the friction joint. Another possible modelling technique consists in

inserting a thin layer of element with nonlinear properties between the flanges. H. Ahmadian, M. Ebrahimi, J.E. Mottershead, M.I. Friswell (2002) [9] have developed several bolted joint finite element model using this technique. The thin layer elements are given material nonlinear properties such as an elastic-plastic behaviour so that it behave in the nonlinear way from a given level of vibrations. This has the ability to fit the nonlinear measured response with a low relative error. However, this usually works for a single mode analysis and the material properties need to be identified using measurement data. The last type of friction joint modelling technique is the use of contact elements at the contact interface of the bolted joint [20]. In a simplified way, the finite element solver projects the vector normal from the surfaces in contact. It then creates contact elements when these normal intersect elements from the facing surface elements. These contact elements are then given friction properties. In our case, we used a glued contact model for the linear model (flange surfaces considered merged) and a coulomb friction model for the nonlinear model. These contact elements are also called phenomenological models as they represent the friction force as a function of the relative displacement between the surfaces in contact. They are Iwan model [7] composed of Jenkins elements (spring element in series with a coulomb element) in parallel. This is the type of nonlinear elements used in the flange structure nonlinear model. These have the advantage of reproducing an accurate vibration response compared to an actual model. However, as it will be further noticed, this type of FEM has the disadvantage of being very computational time consuming. As previously said, the contact elements have many contact properties. The most important ones are the friction model used and the associated friction coefficient. In our case, the Coulomb friction model is chosen as this is the most commonly used in the industry. It is associated with a friction coefficient which is set to 0.3, being an average value for steel against steel friction.

7.3.1.2 Bolts modelling

In the case of contact elements, it is also important to model the effect of bolts on the flange. There are several ways to model the bolts. As it has seen in the previous paragraph, in the case of a linear model, they are usually removed from the model as well as their preload. In the case of a nonlinear model where the joint dynamics are modelled, the pressure applied by the bolt on the flanges is computed by the use of contact elements. The bolts with their associate preload are either modelled with solid elements (nuts and screws) or with the association of beam and rigid elements as it can be seen in Figure 30.

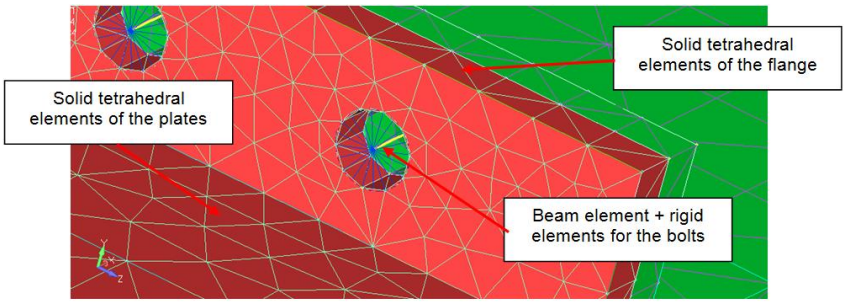

Figure 30 Nonlinear FEM mesh of the flange structure (zoom on the bolted joint)

The later possibility is chosen as it simplifies the model. The preload values need to be the same as used during the measurement process. For the actual bolt tightening, a torque wrench was used and set to a torque value of 10 N.m. The normal bolt preload can be estimated from this tightening torque with the relationship below [21]:

$$P = \frac{T}{K \times d}$$

With:

- T: Tightening torque (10 N.m)
- K: nut factor (estimated to 0.2 according to [21] for steel bolts
- d: Nominal bolt diameter (6 mm)

Then, the calculated preload is $P = 8333\ kN$. This is the value of compression force given to the beam elements modelling the bolts. A static FEA has been performed with only the bolt preloads as an input. The contact pressure on the flange interface is shown in Figure 31.

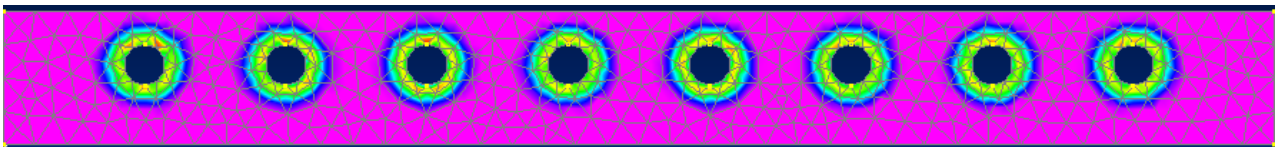

Figure 31 Contact pressure computed by the nonlinear FEM with only the bolt preloads as an input (purple being the min and red the max pressure)

7.3.1.3 Plates and flanges modelling

In the case of dynamic analysis using contact elements, solid elements need to be used for the surfaces being in contact. This is why, all the rest of structure is modelled using solid tetrahedral parabolic elements although it increases a lot the number of elements compared to a shell element model. The associated material properties are:

- Mass density: $\rho = 7800\ kg.m^{-2}$
- Young Modulus: $E = 204955\ Mpa$
- Poisson's ratio: $\nu = 0.3$

7.3.1.4 Boundary conditions and solution type

As we want to reproduce the structural behaviour achieved in the measurements, similar boundary conditions are set. That is to say, the structure itself is in free-free conditions, although the actual wire suspension must have had an impact on the response compared with perfect free-free conditions of the numerical model. The force input is a sinusoidal nodal force at the actual input location. The acceleration, normal and shear components of strain are set as output requests at the actual positions of the sensors. The solution type is an advanced nonlinear transient response. Then, the solver parameters also need to be set. The most important parameters are the time step and the number of steps. Those parameters depend on the force input frequency, the maximum frequency component that we want to capture, the spectral analysis resolution desired, and the transient response time. Several trials and errors have been tested in order to find the best compromise of time step and number of steps for every analysis.

7.3.2 Time-domain results for the critical modes

As previously said, four nonlinear FEA are performed: two per critical mode (with a low and high forcing levels). The forcing levels are set to 5 and 50 N in both cases for respectively the low and high levels. The high value is higher than what had been achieved during the experimental campaign. This is another advantage of performing a numerical analysis, as high level of vibrations can be achieved. The objective is to observe nonlinear features that can be compared between the low and high levels of vibrations. To do so, a similar signal post-process as in the measurement campaign is used with an appropriate *LabView* program. The second type of normalization (b) seen in IV.1.2.2 is used to study the evolution of acceleration and strain harmonics as a function of the excitation level.

7.3.2.1 Mode 4 (T2)

The FE linear natural frequency of mode 4 is 170.2 Hz. Then, this is the chosen value for the excitation force frequency. The band width is set to 1000 Hz in order to capture up to the fifth harmonic of the fundamental frequency. The time step chosen for sampling this mode is $0.0005\ s$. The number of steps is set to 1000, giving a total simulated time of 0.5 s. As said before, the main disadvantage of contact elements in a FEM is their impact on the computational time. Indeed, the total simulation time for one analysis was 6 hours (to simulate 0.5 s of actual behaviour). The time response seems to be in steady state from 0.3 s for the 5 N excitation case. Below are the results of normalized values of acceleration and strain harmonics as a function of the excitation force amplitude. Some interesting features were observed up to the fifth harmonic.

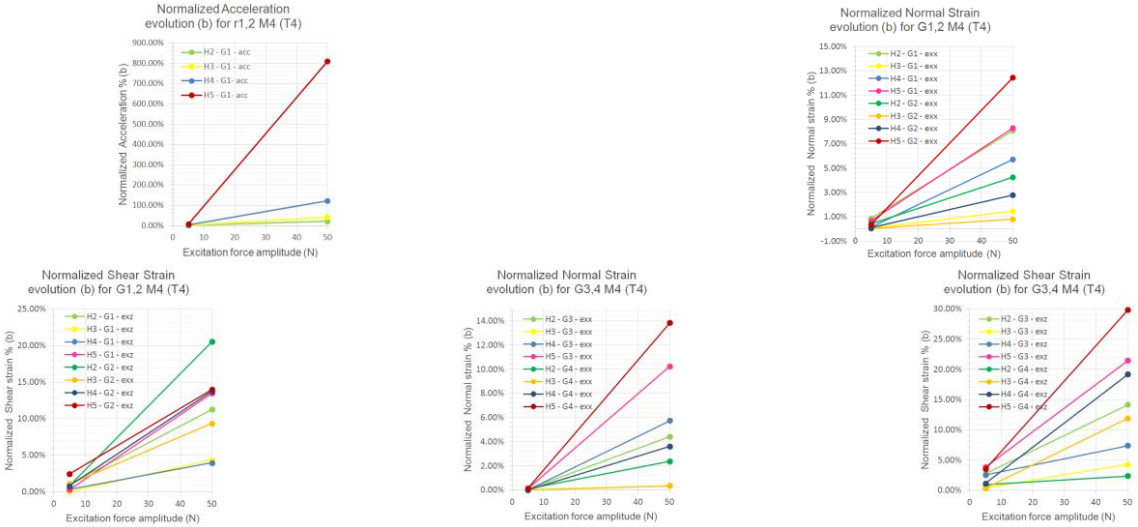

Figure 32 Evolution of the normalized (b) numerical acceleration, normal and shear strains for a low and high levels of excitation forcing of mode 4 (170 Hz)

It can be seen from the normalized acceleration plot that harmonics amplitudes become important for the high forcing level. The fifth harmonic is unexpectedly high (800 % of the fundamental). This is probably due to a too high time step. However, more interesting nonlinear features can be observed on the normalized strain plots. First, almost all relative harmonic amplitudes increase with the level of forcing, showing that the higher the excitation force, the more nonlinearities are caused by the bolted joint. This is especially the case for the fourth and fifth harmonics. There also seems to be some nonlinearity discontinuities between the left and right plate according to the difference in harmonic levels between G1 and G2 or G3 and G4. However, no conclusion can be made about this feature as there is no logical pattern. Sometimes, the harmonic levels on the right plate are higher than the left plate and the other way round. Figure 33 shows a part of the time response of $G4\epsilon_{xz}^2$ with the associated spectral analysis. It is obvious that nonlinearities appear as the time response is not a perfect sinusoidal signal. This is highlighted by the harmonic peaks that are relatively high compared to the fundamental amplitude.

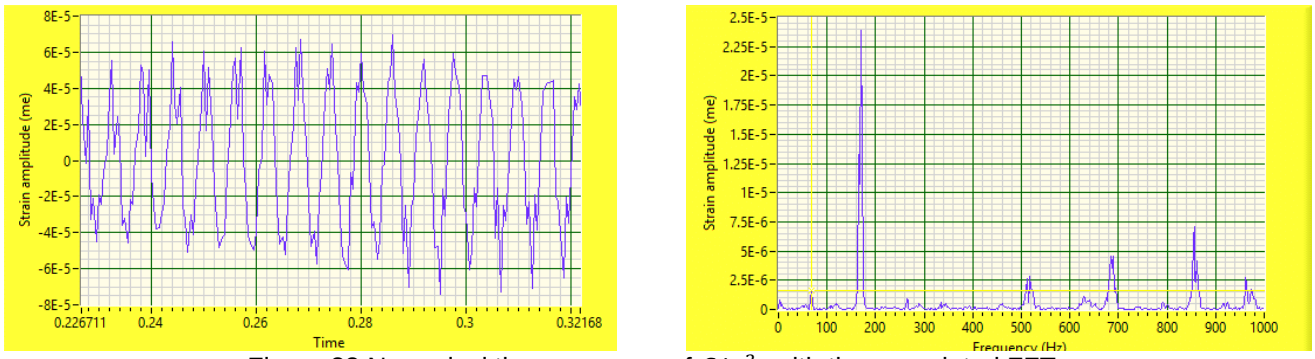

Figure 33 Numerical time response of $G4\epsilon_{xz}^2$ with the associated FFT

7.3.2.2 Mode 8 (T4)

The FE linear natural frequency of mode 8 is 370.8 Hz. Then, this is the chosen value for the excitation force frequency. This time the bandwidth is set up to 2500 Hz in order to capture up to the fifth harmonic of the fundamental frequency and using a time step of $0.0002\ s$. The number of steps is set to 1000, giving a total simulated time of 0.2 s. Figure 34 are the acceleration responses for the low and high excitation forces. It can be noticed that there is an important low frequency component in addition to the fundamental that could be explained by the boundary conditions. Indeed, the FE solver has probably struggled to compute the analysis without any constraints (free-free conditions). However, as for mode 4, we are only interested in the normalized values of harmonics in this analysis. But the nonlinearities can already be highlighted from those graphs since high frequency components appear on the high excitation force plot.

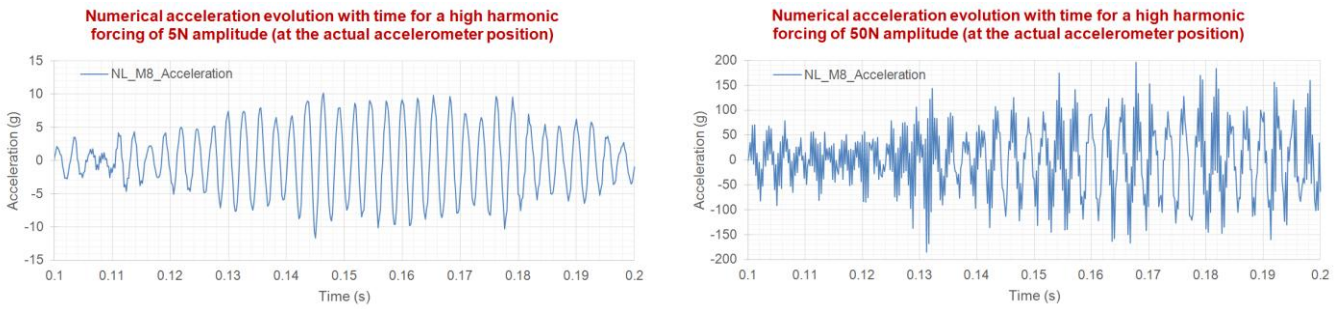

Figure 34 Time domain numerical acceleration evolution of mode 8 (370 Hz) for 5 and 50 N of excitation force amplitudes

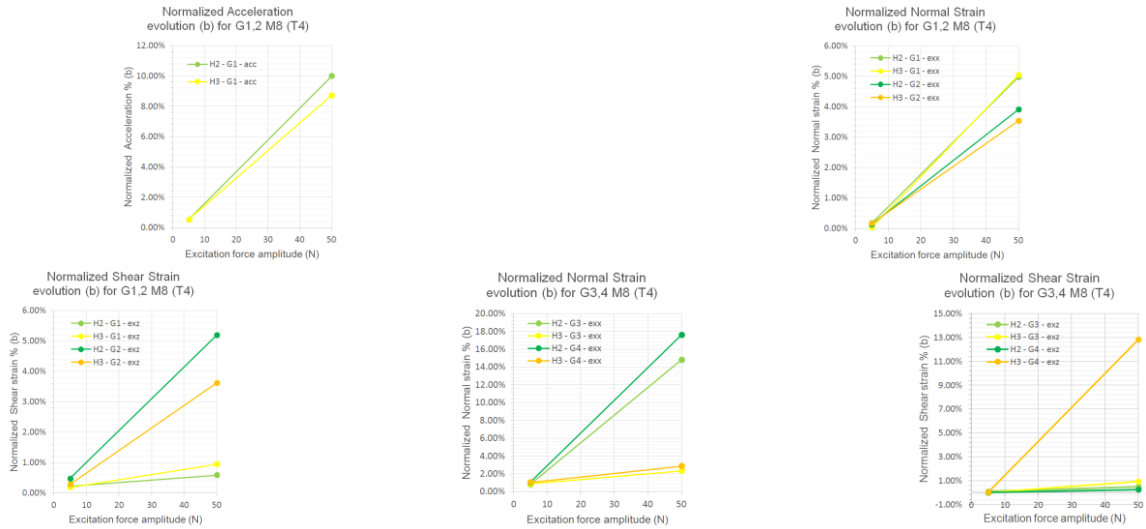

Figure 35 Evolution of the normalized (b) numerical acceleration, normal and shear strains for a low and high levels of excitation force of mode 8 (370 Hz)

As for mode 4, the first interesting trend to observe for almost every curve is the increase in normalized harmonic level with an increasing excitation force level. This shows that the nonlinearity caused by the bolted joint is higher for the high forcing level. This is the case for both acceleration and most strain components for all gauges, showing that strain is also an interesting nonlinearity indicator such as acceleration. The shear strain components of G1 and G2 show a discontinuity between the left and the right plates as $G_2\epsilon^2_{xz\_H2,3} > G_1\epsilon^2_{xz\_H2,3}$. There also seems to be a shear strain discontinuity between G3 and G4 as $G_4\epsilon^2_{xz\_H3} > G_3\epsilon^2_{xz\_H3}$. As a partial conclusion, this FE nonlinear analysis has shown that a FEM containing contact elements with friction properties allows to capture the dynamic nonlinearities induced by a bolted joint. Indeed, the acceleration and strain components outputs show similar nonlinear features than we had been obtained in the experimental analysis. That is to say, a global increase of normalized harmonics with an increasing level of vibrations in the structure for both acceleration and strains. The advantage of the numerical model is its ability to capture some nonlinear features of level of vibrations that could not be achieved using the experimental set up. However, there are several drawbacks in this type of nonlinear Finite Element Model. First, there are a large number of uncertainty sources such as the errors on the friction coefficient, the errors on bolt preloads and the friction model used by the contact elements which is maybe not accurate enough to capture the actual joint behaviour. The mesh size in the contact area is also critical. The other disadvantage is the computational time which can be very large when contact elements are used. In our case, it took more than 6 hours to simulate less than 1 s of structure dynamics.

8 CONCLUSIONS

This paper presented a research work focussed on nonlinear dynamics of bolted flanges. A section of a Rolls-Royce aero-engine casing was redesigned in order to remove several geometrical details but preserving its major dynamic properties. The objective was to study the nonlinear dynamics by measuring and analysing the strains across the flange. The work was dived in several stages each of which assured that the level of knowledge about

the modal characteristics of the components were as complete as possible. So, linear modal analysis was carried out for performing model updating. A ranking of the mode shapes to be tested up to nonlinear vibration was attempted by using strain analysis. This ranking was experimentally validated by performing modal testing under nonlinear conditions and which were executed using different control methods. An FE model of the flange was built using contact elements at the flange location. This enabled the time response analysis and prediction of strains for given excitation mode. The test structure was equipped with strain gauges at four locations across the flange. Nonlinear testing was carried out and strain data acquired and analyzed. Both theoretical and experimental data were correlated. The research showed that strains can be sensitive to nonlinearity even for smaller levels of vibrations than the actual required for accelerometers. The ranking based on strain analysis showed that torsional modes tend to present more nonlinearity than the bending ones. Additional work must be carried out in this direction. Specifically, in the area of nonlinear response prediction of FE models. This is still base on numerical integration which is very time consuming and therefore limiting the data generation and analysis.

References

[1] D. J. Ewins, “Modal Testing theory, practice and applications” – second edition – RSP editor.
[2] C. Blandin (2013): “Identification of dynamic nonlinearities of bolted structures” – MSc Project literature review report from the University of Bristol
[3]: R.A. Ibrahim and C.L. Pettit (2003): “Uncertainties and dynamic problems of bolted joints and other fasterners”. Journal of Sound and Vibration 279 (2005)
[4]: Y. Song, D. McFarland, A. Bergman, F. Vakakis (2005): “Effect of Pressure Distribution on Energy Dissipation in Mechanical Lap Joint”. AIAA JOURNAL - Vol. 43, No. 2, February 2005
[5]: S. Bograd, P.Reuss, A.Schmidt, L.Gaul, M.Mayer (2010): “Modeling the dynamics of mechanical joints”. Mechanical Systems and Signal Processing 25 (2011) p. 2801–2826
[6]: D. Di Maio, C. Schwingshackl, I. Sever: “Development of a test planning methodology for performing experimental model validation of bolted flanges”
[7]: M. Oldfield, H. Ouyang, E. Mottershead (2004): “Simplified models of bolted joints under harmonic loading”. Computers and Structures 84 (2005) p. 25–33
[8]: L. Gaul and J. Lenz (1997): “Nonlinear dynamics of structures assembled by bolted joints”. Acta Mechanica 125, p. 169-181 (1997)
[9]: H. Ahmadian, M. Ebrahimi, J.E. Mottershead, M.I. Friswell (2002): “Identification of bolted-joint interface models” - Proceedings of ISMA2002 - volume IV p. 1741-1748
[10]: M. Böswald, M.Link: “Identification of Nonlinear Joint Parameters by using Frequency Response Residuals”. University of Kassel (Germany)
[11]: B. Cazzolato, S. Widly, J. Codrington, A. Kotousov, M. Schuessler (2008): “Scanning laser vibrometer for non-contact three-dimensional displacement and strain measurements”. From Proceedings of ACOUSTICS 2008
[12]: E. Chatelet, T. Baranger, G. Jacquet-Richardet, A. Saulot (2014): “Identification of contact area from full-field displacement surface measurements”. Proceedings of ASME Turbo Expo 2014 – GT2014-25504
[13]: C. Blandin (2014): “Design and Finite Element linear modal analysis of a simplified aircraft engine casings assembly and research proposal for a methodology for performing the identification of dynamic nonlinearities of a flange bolted structure” – From the University of Bristol
[14]: Billings, S. A. (2013). “Nonlinear System Identification: NARMAX Methods in the Time, Frequency, and Spatio-Temporal Domains”. Wiley. ISBN 978-1-118-53556-1.
[15]: M. Pastor, M. Binda, T. Harcarik: “Modal Assurance Criterion”. Procedia Engineering 48 (2012) 543 – 548.
[16]: Wagg, D.J. & Nield S. A.: “Nonlinear vibration with control”. Springer 2009.
[17]: Vishay Precision Group (2010): “Strain Gage Rosettes: Selection, Application and Data Reduction”. Tech Note TN-515
[18]: A. Herzog, M. Krack, L. Scheidt and J. Wallascheck (2014): “Comparison of two widely-used frequency-time domain contact models for the vibration simulation of shrouded turbine blades”. Proceedings of ASME Turbo Expo 2014 – GT2014-26226.
[19]: A. Jensen (2010): “Linear Contact Analysis: Demystified”. Finite Element Analysis Predictive Engineering.
[20]: K. H. Brown, C. Morrow, S. Durbin and A. Baca (2008): “Guideline for Bolted Joint Design and Analysis: Version 1.0”. Sandia National Laboratories.
[21]: “ICATS.” ICON Suite, 58 Prince’s Gate Exhibition Road, London SW7 2PG.
[22]: “FEMtools”. Dynamic Design Solutions N.V. (DDS) Interleuvenlaan 64, B-3001, Leuven, Belgium

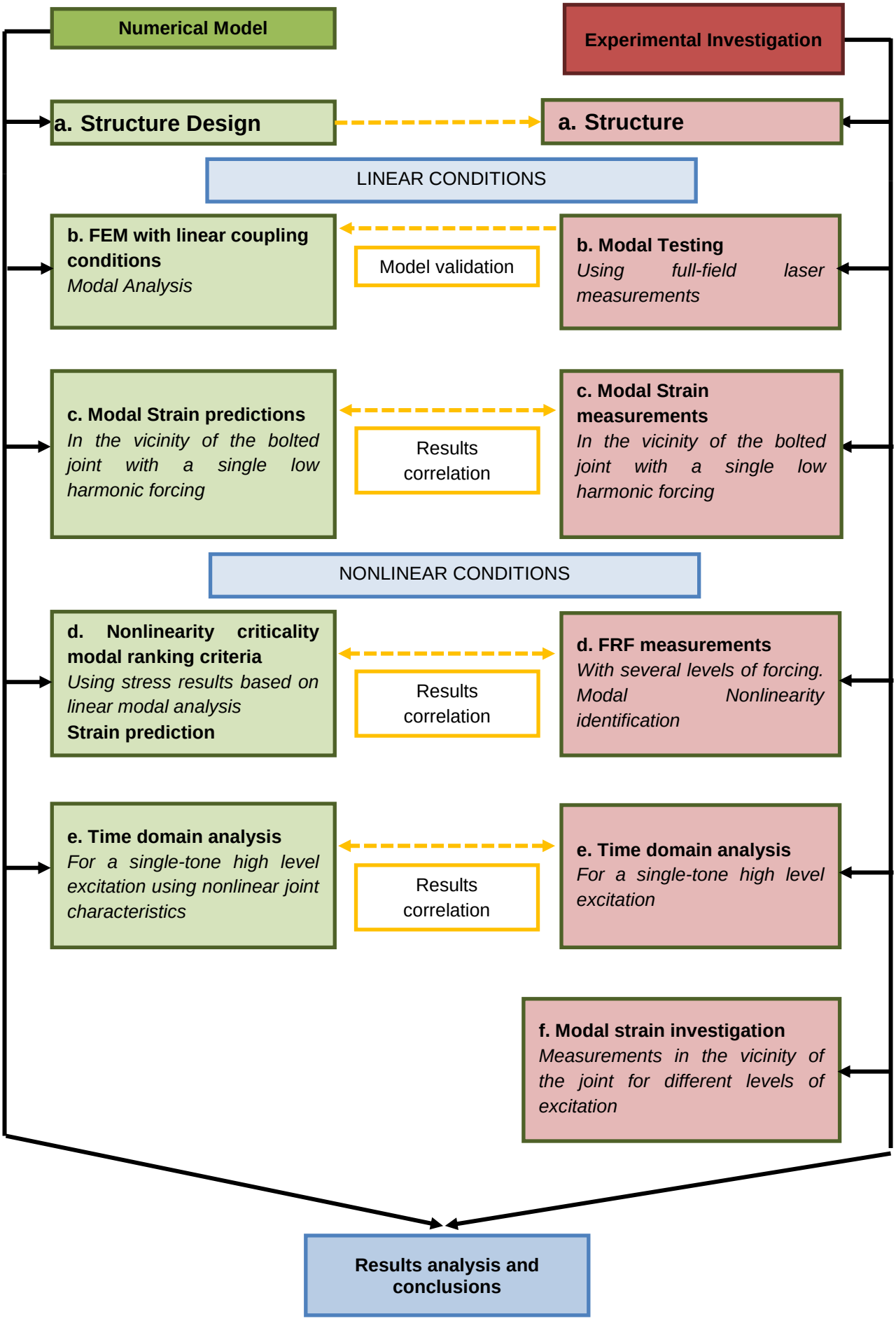

Figure 36 Schematic of the project